JOURNAL OF COLLOID AND INTERFACE SCIENCE 174, 456–460 (1995)

Fractal Cluster Size Distribution Measurement Using Static Light Scattering

C. M. SORENSEN,[1] N. LU, AND J. CAI

Department of Physics, Kansas State University, Manhattan, Kansas 66506-2601

Received November 10, 1994; accepted March 9, 1995

We present a method which uses the behavior of the scattered light intensity as a function of the scattering wave vector in the Guinier to power law crossover regime to determine the width of the size distribution of fractal cluster aggregates. A graphical analysis is presented and data for soot aggregates is used to illustrate the method. This analysis relies upon knowledge of the fractal cluster dimension and correlation function cutoff, and we discuss how uncertainties in these parameters lead to uncertainties in the size distribution width. © 1995 Academic Press, Inc.

Key Words: **fractals; size distribution measurement; light scattering.**

I. INTRODUCTION

Optical particle sizing is a valuable technique for *in situ,* noninvasive diagnostics of particulate systems. The desired information is a complete description of the particle size distribution, but this can be very difficult to obtain. Practically, we are satisfied with accurate mean size information and some degree of knowledge regarding the nature of the distribution, usually its width. In this paper we describe a graphical method to obtain the size distribution width of fractal aggregates via light scattering measurements which we have found useful in our studies of soot aerosols.

The scattering of light, or any other wave, from particles or clusters can be divided into three regimes (1–3) based on the magnitude of qR_g where R_g is the particle or cluster radius of gyration and $q = 4\pi\lambda^{-1}\sin\theta/2$, where λ is the radiation wavelength and θ is the scattering angle, is the scattering wave vector. These regimes are the Rayleigh regime where $qR_g \ll 1$, in which the scattered intensity is constant, independent of the scattering angle; the Guinier regime where $qR_g < 1$, in which a small angle dependence is seen due to the overall size of the particle; and, typically, a power law regime for $qR_g > 1$, in which the intensity angular dependence contains information regarding the particle's or cluster's structure.

The particle or cluster mean size can be obtained in the Guinier regime where

$$I(q) = I(0)(1 - q^2R_g^2/3) \qquad [1]$$

for $qR_g < 1$. In Eq. [1], $I(q)$ is the scattered intensity at wave vector q. Equation [1] holds regardless of refractive index or morphology and hence is very useful for determining cluster or particle size through R_g. It has seen wide spread application (1–6).

We have used Eq. [1] to determine R_g values for soot aerosols (4–6). We found it conceptually useful to plot the inverse, normalized scattered intensity, $I(0)/I(q)$, versus q^2 because such graphs should be linear with a slope of $R_g^2/3$ and remain quite linear even when $qR_g > 1$. This plot is similar to a Zimm plot (7, 8) except that no cluster concentration extrapolation is carried out since our soot clusters are near zero concentration. The linearity for $qR_g > 1$ puzzled us because Eq. [1] should only hold for $qR_g < 1$ and plots of the complete structure factor begin to curve severely for $qR_g > 1$. Further numerical analysis showed that inclusion of polydispersity lessened this curvature and that the transition from the Guinier to the power law regime, i.e., as qR_g passed through unity, was sensitive to a number of details regarding the morphology of the individual clusters and, most importantly for our purposes here, the cluster size distribution. A subsequent review of the literature showed that this knowledge was not new. Shull and Roess (9) used graphical methods, different than those we will present here, to show for a system of spheroidal particles how the Guinier to power law, which for spheroids is a q^{-4} Porod law, transition is sensitive to the size distribution of spheroidal particles. Schmidt and co-workers (10, 11) showed how Fourier inversion of small angle X-ray scattering data in this regime could yield the particle size distribution. A disadvantage was that the shape of the particles, e.g., eccentricity, also affected scattering in this regime and hence could confuse the size distribution determination. All of this work was for uniform density, spheroidal particles, i.e., no aggregates. Thus, the usefulness of this crossover regime for size distribution measurements for fractal aggregate clusters remains to be explored. That is the purpose of this paper. We will show that if the morphology of the aggregate is well known, an effective measurement of the size distribution width can be made. Uncertainty in the morphology, however, can seriously limit

[1] To whom correspondence should be addressed.

0021-9797/95 $12.00

the accuracy of this measurement. Our method will be a graphical analysis of the shape of curves plotted in accord with Eq. [1].

II. ANALYSIS

A. *Scattering and the $qR_g < 1$ Regime*

We consider a noninteracting ensemble of clusters with monomers small enough to be Rayleigh scatterers. For such a system, intracluster multiple scattering is not a significant fraction of the scattering (12, 13). We assume the cluster number density is small enough so that there is no intercluster multiple scattering. These conditions are commonly satisfied for many colloidal and aerocolloidal systems. In general, the scattered light intensity from an ensemble of clusters with various numbers of monomers per cluster N and size distribution $n(N)$ is

$$I(q) = c \int n(N) N^2 S(qR_g) dN. \qquad [2]$$

In Eq. [2], c is a constant including functions of the refractive index, collection solid angle, detector efficiency, etc. $S(qR_g)$ is the static structure factor of the cluster. For fractal clusters, $N \sim R_g^{D_f}$ where D_f is the fractal dimension. Since $S(qR_g) = 1$ as $qR_g \to 0$, one may eliminate c to obtain

$$I(q)/I(0) = \frac{\int n(N) N^2 S(qR_g) dN}{\int n(N) N^2 dN}. \qquad [3]$$

In the Guinier regime, $qR_g < 1$, the structure factor is given by $S(qR_g) \simeq 1 - q^2 R_g^2/3$, and this may be substituted into [3]. We define the moments of the size distribution by

$$M_i = \int N^i n(N) dN. \qquad [4]$$

Then Eq. [3] becomes (5)

$$I(q)/I(0) = 1 - (1/3) q^2 a^2 k_0^{-1/D_f} M_{2+2/D_f}/M_2. \qquad [5]$$

In Eq. [5] we have used $N = k_0 (R_g/a)^{D_f}$ where a is the monomer radius and k_0 is a constant. Equation [5] shows that a measurement of R_g obtained by studying the q dependence of the light scattered in the Guinier regime yields an average radius of gyration related to the moments of the distribution by

$$\langle R_g^2 \rangle = a^2 k_0^{-2/D_f} M_{2+2/D_f}/M_2. \qquad [6]$$

The functional dependence of the Guinier formula may be used to find average R_g values. A convenient graphical method is to plot the inverse of the scattered intensity, $I(0)/I(q)$, versus q^2. Then the slope is $1/3 \langle R_g^2 \rangle$. We used inverse $I(q)$ because $I^{-1}(q)$ is not bounded whereas $I(q)$ is, hence $I^{-1}(q)$ versus q^2 tends to be more linear and easier to analyze. An example for a soot aerosol is shown in Fig. 1, which has been used to yield accurate R_g values (4).

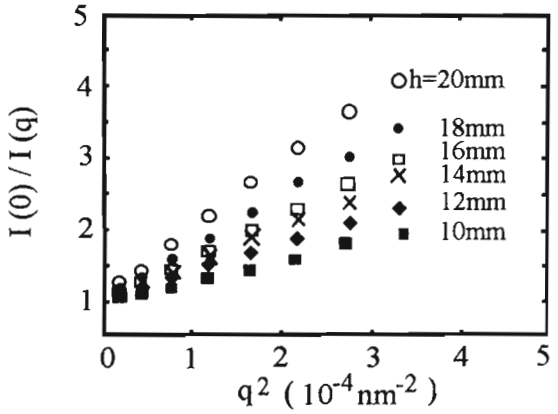

FIG. 1. Normalized inverse scattering intensity versus wave vector squared for light scattered from soot aggregates in a premixed CH_4/O_2 flame. The parameter h is the height above the burner surface from which the data were obtained. Linearity is in accord with the Guinier approximation, Eq. [1], and the slopes are $\langle R_g^2 \rangle/3$.

A close look at Fig. 1 shows that we have used data for which $qR_g > 1$, beyond the Guinier regime, yet $I^{-1}(q)$ versus q^2 is still surprisingly linear. Linearity is expected only for $qR_g < 1$. This curious fact and our desire to understand the effect of $n(N)$ on these plots led us to realize that the $qR_g \gtrsim 1$ region of these graphs is very sensitive to the functions that go into Eq. [2], the functions $n(N)$ and $S(qR_g)$.

B. *The $qR_g \gtrsim 1$ Regime*

Two major parameters determine the form of $S(qR_g)$ for a cluster. They are the fractal dimension D_f and the cutoff function of the cluster density–density correlation function. The fractal dimension essentially determines the limiting slope as $S(qR_g) \sim (qR_g)^{-D_f}$ for $qR_g \gg 1$ regardless of the cutoff function. For diffusion limited cluster aggregates (DLCA) $D_f \sim 1.7$ to 1.8. The fractal dimension is readily measured if $qR_g \gg 1$ data are available, and it is still measurable if not, provided one knows about the cutoff function and the size distribution (6).

The density correlation function $g(r)$ may be written as (6, 14)

$$g(r) \sim r^{D_f - d} h(r/\xi), \qquad [7]$$

where d is the spatial dimension. The cutoff function is $h(r/\xi)$ where ξ is a characteristic cluster size related to R_g. It describes the manner in which the density of the cluster terminates at the perimeter. It is important because $S(qR_g)$ is the Fourier transform of $g(r)$. Regardless of $h(r/\xi)$,

$S(qR_g)$ will have the same Rayleigh and Guinier ($qR_g < 1$) and power law ($qR_g \gg 1$) limits. It is the shape of the Guinier to power law crossover regime $qR_g \geq 1$ that is affected by $h(r/\xi)$.

The problem is, what is $h(r/\xi)$? Most earlier workers used an exponential $h(r/\xi) = \exp[-r/\xi]$ (15, 16). Mountain and Mulholland (17) created simulated clusters and found $h(r/\xi) = \exp[-(r/\xi)^{\beta}]$ with $\beta = 2.5 \pm 0.5$. A reasonable physical mechanism for the cutoff can be obtained by considering two overlapping spheres, which yields $h(r/\xi) = (1 + r/4\xi)(1 - r/2\xi)^2$, $r < 2\xi$, otherwise zero (2, 18).

We have studied $h(r/\xi)$ in two different ways. First, we compared measured structure factors from soot to various structure factors derivable from the different cutoffs (6). We found the most reasonable fits were obtained for a structure factor derivable from a Gaussian cutoff, $h(r/\xi) = \exp[-(r/\xi)^2]$. Second, we captured soot particles on electron micrograph grids, photographed them with the electron microscope, computer digitized their images, and then calculated $g(r)$ from which $h(r/\xi)$ was determined directly (14). We found both the Gaussian cutoff and the overlapping spheres cutoff described the data accurately. These two cutoffs are nearly identical in the range $h(r/\xi) \geq 0.01$. Given our empirical evidence for a Gaussian cutoff and the physical reasoning that leads to the overlapping sphere cutoff and their essential equivalence, we shall use a structure factor derivable from the Gaussian cutoff (the overlapping sphere cutoff does not allow for an analytic expression for $S(qR_g)$) which is

$$S(qR_g) = e^{-(qR_g)^2/D_f}\,{}_1F_1\left(\frac{3 - D_f}{2}, \frac{3}{2}; \frac{(qR_g)^2}{D_f}\right), \quad [8]$$

where ${}_1F_1$ is the confluent hypergeometric series.

The other functionality in Eq. [3] is the size distribution, $n(N)$. Since our method will not yield $n(N)$ directly, the best to which we can aspire is to measure an effective width. Thus a functional form for $n(N)$ must be assumed which will have a width parameter. In this work we have used two different size distribution functional forms: the Zeroth Order Log Normal (ZOLD) (1, 19) and the scaling distribution (20).

The functional form for the normalized ZOLD is

$$n(N) = (\sqrt{2\pi} N_0 \ln \sigma_N \exp[+1/2 \ln^2 \sigma_N])^{-1} \times \exp\left\{\frac{-\ln^2 N/N_0}{2 \ln^2 \sigma_N}\right\}. \quad [9]$$

N_0 is the most probable "size," number of monomers per aggregate, and σ_N is the geometric width in N-space. Note that conversion to radius space requires $\sigma_R = \sigma_N^{1/D_f}$. We will show that the curvature of our $I(0)/I(q)$ versus q^2 graphs is dependent on σ_N, hence it can be measured.

The normalized scaling distribution is given by

$$n(N) = M_1 s^{-2} \Phi(x) \quad [10a]$$

$$\Phi(x) = \alpha^{\alpha} \Gamma^{-1}(\alpha) x^{-\lambda} e^{-\alpha x} \quad [10b]$$

$$x = N/s. \quad [10c]$$

In Eqs. [10], $s = M_1/M_0$ a mean size, $\alpha = 1 - \lambda$, and Γ is the Gamma function. The effective width parameter is λ, and the bigger λ the broader the distribution. Equations [10] are good only for the large x tail of the distribution ($x \geq 1$). This is all we need for light scattering, however, since the scattering weights the large x tail. This is seen in Eq. [3] and is due to the N^2 term. In fact it's all we can get from light scattering which is blind to the small x part of the distribution.

Both these distributions have various attributes. The ZOLD is intuitively reasonable and is popular in the engineering community. It can be used to describe nearly any ensemble of particles or clusters. It can also do a good job of approximating the self preserving size distributions that result from aggregation. The scaling distribution is an exact description of the self preserving size distributions and λ is the aggregation kernel homogeneity. The apparent disadvantage of having the wrong small size limit is unimportant since essentially all of the mass or, in our case, all of the light scattered is due to the large size part. This approach is popular in the physics literature. We have preferred the scaling distribution because it accurately describes moments higher than the second which become important for interpreting light scattering measurements (5), for example Eq. [6] shows $\langle R_g^2 \rangle \sim M_3/M_2$ for $D_f \sim 2$. In describing self preserving distributions, the two distributions yield identical first and second moments when

$$(2 - \lambda)/(1 - \lambda) = \exp[\ln^2 \sigma_N], \quad [11]$$

for $\lambda < 1$. This rough equivalence will be seen in our results below.

III. RESULTS

Equation [3] was used to calculate the normalized scattered intensities from an ensemble of clusters with fractal dimension $D_f = 1.75$, typical of DLCA clusters. The single cluster structure factor was that due to a Gaussian cutoff, Eq. [8]. Both the ZOLD and the scaling distributions were used with a series of different width parameters, σ_N and λ, respectively. The intensity was inverted to $I(0)/I(q)$,

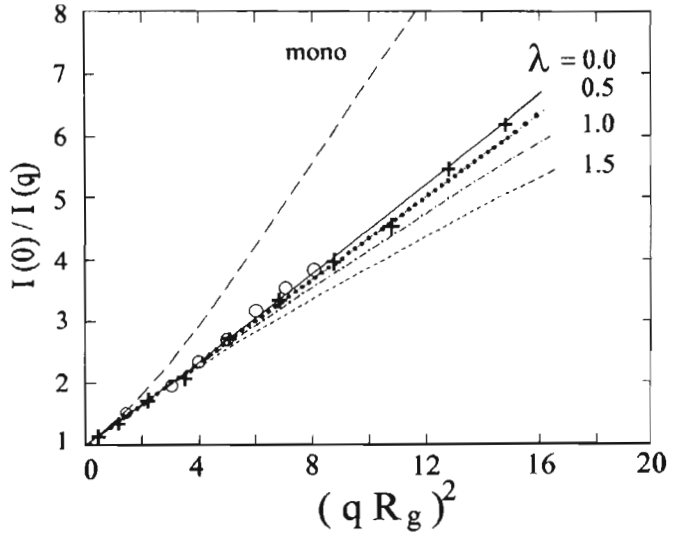

FIG. 2. Normalized inverse scattering intensity versus the product of the wave vector and the cluster radius of gyration quantity squared for various values of the scaling distribution width parameter, $D_f = 1.75$, and a structure factor derived from a Gaussian cutoff correlation function. Curves were calculated from Eq. [3]. Data points are for a premixed CH_4/O_2 flame at height above burner: (○) $h = 12$ mm; (+) $h = 18$ mm.

plotted versus $(qR_g)^2$ and the results are shown in Figs. 2 and 3.

Figures 2 and 3 readily show that the curvature (or lack of it) in these graphs is a function of the distribution width when $qR_g > 1$. Note how inclusion of a finite width drastically lessens the curvature compared to the monodisperse case (Fig. 2). Data for scattering from a soot aerosol at two different heights above the burner of a C/O = 0.75 premixed CH_4/O_2 flame are also shown in these figures and one can see a measurement of the width as either $\lambda = 0.2 \pm 0.3$ or $\sigma_N = 2.3 \pm 0.3$. These two values roughly fit with Eq. [11]. When $qR_g < 1$, all the curves lie together as expected for the Guinier regime.

Thus we propose the following method for measurement of mean size and size distribution width for an aerosol or colloid. Relative intensity is measured as a function of wave factor q at several q values, most conveniently by changing the scattering angle. The fractal dimension is either determined from the large qR_g power law behavior (5), other more esoteric means (5), or assumed from the possibly known aggregation kinetics. Plot $I(q)^{-1}$ versus q^2; the limiting $q \to 0$ slope yields $1/3\ \langle R_g^2 \rangle$ via the Guinier equation, and the data can be accurately extrapolated to $q = 0$ to yield $I(0)$. Replot as $I(0)/I(q)$ versus $(qR_g)^2$ and compare the data to the curves in Figs. 2 and 3 as easily calculated by Eq. [3]. Read off the value of the width parameter. Appendix A describes the mathematical detail in calculating Eq. [3] for a given R_g.

Perhaps the greatest asset of this method is its simplicity. Problems arise, however, in the sensitivity of these curves to other factors in the single cluster structure factor, the fractal dimension D_f and the cutoff function. These problems are analogous to spheroid shape effects for noncluster particles in the earlier work (9–11). We illustrate these sensitivities next.

Figure 4 shows $I(0)/I(q)$ versus $(qR_g)^2$ for a scaling distribution with $\lambda = 0$ and a Gaussian cutoff structure factor with various D_f. We see the curvature in these graphs is sensitive to D_f. Fortunately, D_f is readily measurable. Com-

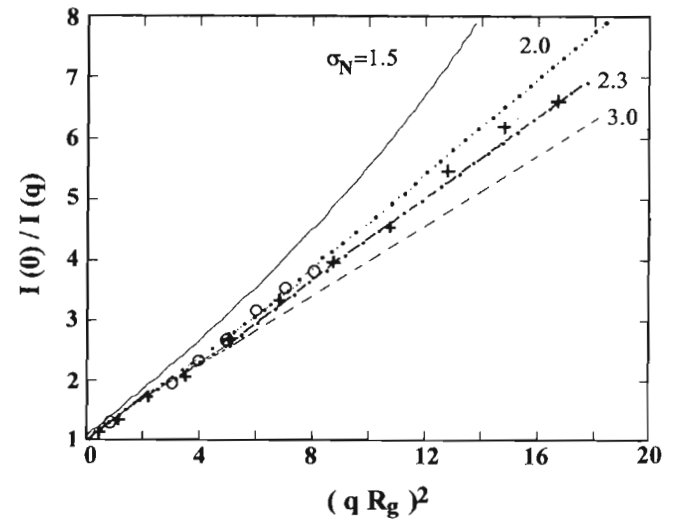

FIG. 3. Normalized inverse scattering intensity versus the product of the wave vector and the cluster radius of gyration quantity squared for various values of the ZOLD width parameter, $D_f = 1.75$, and a structure factor derived from a Gaussian cutoff correlation function. Data points are for a premixed CH_4/O_2 flame at height above burner: (○) $h = 12$ mm; (+) $h = 18$ mm.

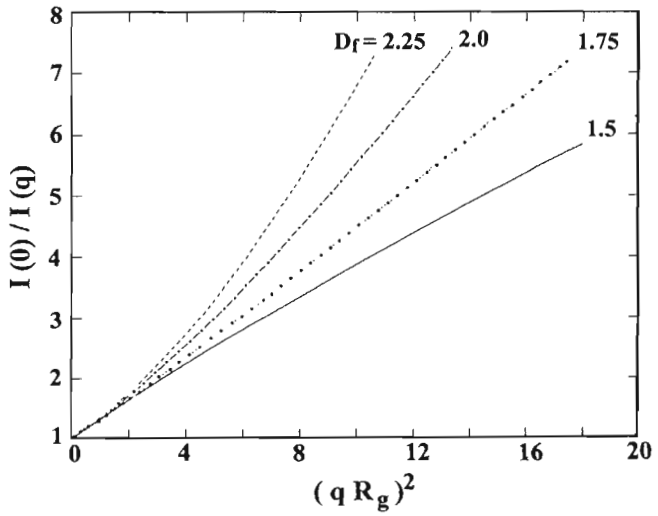

FIG. 4. Normalized inverse scattering intensity versus the product of the wave vector and the cluster radius of gyration quantity squared for a scaling distribution with width parameter $\lambda = 0$, a structure factor derived from a Gaussian cutoff correlation function, and various values of the fractal dimension.

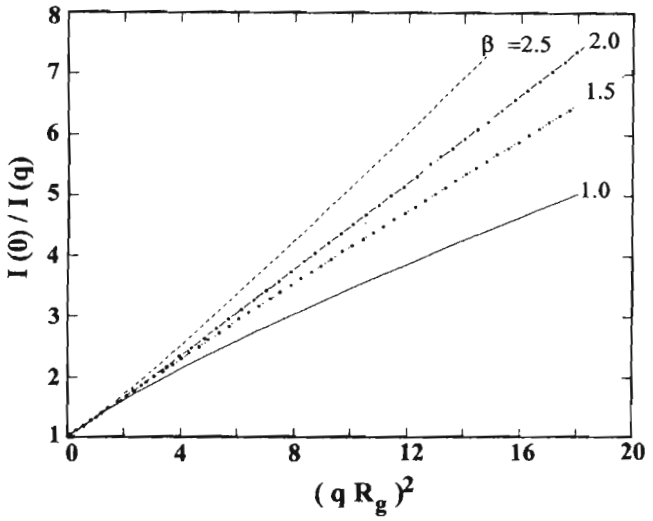

FIG. 5. Normalized inverse scattering intensity versus the product of the wave vector and the cluster radius of gyration quantity squared for a scaling distribution with width parameter $\lambda = 0$, a structure factor derived from a correlation function with various values of β for the cutoff function, and a fractal dimension of $D_f = 1.75$.

parison of Figs. 2 and 4 suggests that an uncertainty of ± 0.05 in D_f, a typical value, leads to an uncertainty of ± 0.3 in the λ inferred via our procedure.

We may represent the density correlation cutoff function as a generalized exponential

$$h(r/\xi) = \exp[-(r/\xi)^{\beta}]. \qquad [12]$$

The parameter β is the stretching parameter and $\beta = 2$ for a Gaussian. In Fig. 5 we plot $I(0)/I(q)$ versus $(qR_g)^2$ for a scaling distribution with $\lambda = 0$ and a structure factor with $D_f = 1.75$ and cutoff given by Eq. [12] for various β. We see the curvature of these graphs is sensitive to β. Unfortunately this parameter is not readily measured. We feel, however, that our value of $\beta = 2.0$ is quite good given our past work on this parameter and its similarity with the exact overlapping sphere calculation.

IV. CONCLUSIONS

We have shown for fractal clusters that scattering in the crossover region from the Guinier to power law regimes is sensitive to the width of the cluster size distribution. We have shown how this can be used to measure this width. We have also shown that since this crossover is sensitive to individual cluster morphological parameters through the cluster structure factor, these parameters must be well known to allow an accurate measurement of the width. Our work here is an extension of earlier work involving nonaggregated particles.

APPENDIX A

The slope of $I(0)/I(q)$ versus q^2 is $\langle R_g^2\rangle/3$ where $\langle R_g^2\rangle$ is given by Eq. [5]. The moment ratio in [5] is related to the mean sizes of the scaling distribution to yield

$$\langle R_g^2\rangle = s^{2/D_f} a^2 k_0^{-2/D_f} \alpha^{-2/D_f} \Gamma(\alpha + 2 + 2/D_f)/\Gamma(\alpha + 2). \qquad [A1]$$

Similarly for the ZOLD distribution,

$$\langle R_g^2\rangle = N_0^{2/D_f} a^2 k_0^{-2/D_f} e^{2(3D_f+1)D_f^{-2}} \ln^2 \sigma_N. \qquad [A2]$$

Thus the mean size s or most probable size N_0 can be found from the R_g measurement.

To calculate the curves in Figs. 2–5, either Eq. [A1] or [A2] is inverted to obtain s or N_0. Then Eq. [3] is used with the dimensionless variable $x = N/s$ or N/N_0. Upon this substitution all the constants in Eqs. [A1] and [A2], such as a, k_0, α, and D_f, cancel out. The structure factor becomes the function $S(q\sqrt{\langle R_g^2\rangle}x^{1/D_f})$, where $\langle R_g^2\rangle$ was from the Guinier measurement. The result from [3] is thus not dependent upon the various unknown constants and can be plotted versus $q\sqrt{\langle R_g^2\rangle}$, nominally "$qR_g$" in Figs. 2–5.

ACKNOWLEDGMENT

This work was supported by NSF Grants CTS9024668 and CTS9408153.

REFERENCES

1. Kerker, M., "The Scattering of Light and Other Electromagnetic Radiation." Academic Press, New York, 1969.
2. Glatter, O., and Kratky, O., "Small Angle X-Ray Scattering." Academic Press, New York, 1982.
3. Martin, J. E., and Hurd, A. J., *J. Appl. Crystallogr.* **20,** 61 (1987).
4. Gangopadhyay, S., Elminyawi, I., and Sorensen, C. M., *Appl. Opt.* **25,** 4859 (1991).
5. Sorensen, C. M., Cai, J., and Lu, N., *Appl. Opt.* **31,** 6547 (1992).
6. Sorensen, C. M., Cai, J., and Lu, N., *Langmuir* **8,** 2064 (1992).
7. Zimm, B. H., *J. Chem. Phys.* **16,** 1099 (1948).
8. Pecora, R., and Berne, B. J., "Dynamic Light Scattering." Wiley, New York, 1976.
9. Shull, C. G., and Roess, L. C., *J. Appl. Phys.* **18,** 295, 308 (1947).
10. Letcher, J. H., and Schmidt, P. W., *J. Appl. Phys.* **37,** 649 (1966).
11. Brill, O. L., Weil, C. G., and Schmidt, P. W., *J. Colloid Interface Sci.* **27,** 479 (1968).
12. Nelson, J., *J. Mod. Opt.* **36,** 1031 (1989).
13. Lu, N., and Sorensen, C. M., *Phys. Rev. E* **50,** 3109 (1994).
14. Cai, J., Lu, N., and Sorensen, C. M., *J. Colloid Interface Sci.* **171,** 470 (1995).
15. Freltoft, T., Kjems, J. K., and Sinha, S. K., *Phys. Rev. B* **33,** 269 (1986).
16. Berry, M. V., and Percival, I. C., *Opt. Acta* **33,** 577 (1986).
17. Mountain, R. D., and Mulholland, G. W., *Langmuir* **4,** 1321 (1988).
18. Hurd, A. J., and Flower, W. L., *J. Colloid Interface Sci.* **122,** 178 (1988).
19. Lee, K. W., *J. Colloid Interface Sci.* **92,** 315 (1983).
20. van Dongen, P. G., and Ernst, M. H., *Phys. Rev. Lett.* **54,** 1396 (1985).